Acta Mech 226, 4207–4221 (2015)
DOI 10.1007/s00707-015-1457-5

ORIGINAL PAPER

Peijian Chen · Shaohua Chen · Juan Peng

Frictional contact of a rigid punch on an arbitrarily oriented gradient half-plane

Received: 28 May 2015 / Revised: 13 August 2015 / Published online: 7 September 2015

Abstract Frictional contact of a rigid punch on a half-plane with shear modulus varying according to an exponential gradient in an arbitrary direction is investigated in this paper. Fourier integral transform method is employed to reduce the current sliding contact problem to a Cauchy-type singular integral equation of the second kind. The contact pressure and the in-plane stress, as well as the stress singularity and the stress intensity factor near both contact edges are obtained, which are further analyzed for different friction coefficients, non-homogeneity parameters and gradient orientation angles. The moment in order to keep the punch moving perpendicularly to the contact surface is also evaluated. All the present results should be helpful for the design of surfaces with strong wear resistance and understanding the mechanical mechanism of graded materials in nature.

1 Introduction

Functionally graded materials (FGMs) generally consist of several constitutes with a graded variation in the volume fractions from one location to the other [1,2]. As an alternative to the conventional homogeneous materials, FGMs tend to reduce mismatching stresses, increase the bonding strength, improve surface properties and provide protection against thermal or chemical environments [3]. Currently, applications of FGMs involving contact with loads transfer between or among different surfaces or interfaces of solids have been drawing great attention from various scientists, generally with friction, such as cylinder linings, brake disks and other automotive components for the purpose of improving the wear resistance [4]. The improved tribological characteristics of FGMs paved the way for their potential use in technological applications such as joint prostheses and high-performance cutting tools [5].

Various studies have indicated that tuned gradients in mechanical properties of compositions and structures offer unprecedented opportunities for the design of surfaces with improving resistance to contact deformation and damage [6–8]. Indentation problems to characterize local properties of FGMs were studied theoretically and experimentally by Suresh et al. [9], Jorgensen et al. [10] and Krumova et al. [11]. Giannakopoulos and Pallot [12] provided a closed-form analytical solution for the two-dimensional contact model of a rigid punch

P. Chen (✉)
School of Mechanics and Civil Engineering, State Key Laboratory for Geomechanics and Deep Underground Engineering, China University of Mining and Technology, Xuzhou 221116, Jiangsu, China
E-mail: chen_peijian@hotmail.com; chenpeijian@cumt.edu.cn

S. Chen (✉)
LNM, Institute of Mechanics, Chinese Academy of Sciences, Beijing 100190, China
E-mail: shchen@LNM.imech.ac.cn; chenshaohua72@hotmail.com

J. Peng
Department of Physics, China University of Mining and Technology, Xuzhou 221116, Jiangsu, China

on a graded elastic substrate and demonstrated that proper gradient variation of the elastic modulus could significantly change the stress distribution around the indenter and alleviate the Hertzian crack at the contact edges. Sliding contact problems of homogeneously elastic substrates coated with FGMs have been studied by Guler and Erdogan [2,4]. Dag and Erdogan [13], Choi and Paulino [14] tackled the contact problem between a sliding rigid punch and a graded substrate with a surface/interface crack. Receding contact between a functionally graded coating and a homogeneous substrate as well as the partial slip contact problem was investigated by El-Borgi et al. [15,16]. Wang et al. analyzed systematically the plane [17], axisymmetric [18] contact problems of FGMs with a linear multilayered model. Inspired by elastic homogeneous models [19,20], the present authors investigated the contact behavior of a functionally graded medium with finite thickness and found significant differences between the model of a half-plane and that of a finite solid [21–23].

As for contact models of graded materials considering interface adhesion, a plane strain adhesive contact model between a rigid cylinder and a graded elastic half-plane was discussed by Chen et al. [24]. A closed-form analytical solution of a rigid sphere contacting with a graded elastic half-space was successfully given by Chen et al. [25]. A further non-slipping adhesive contact model of FGMs was reasonably analyzed by Guo and his coauthors [26–29].

In all the above-mentioned studies, graded properties of materials are assumed to vary along the thickness direction, which is perpendicular to the contact interface; few works consider FGMs with gradient in lateral directions [30]. However, materials with gradient properties in an arbitrarily oriented direction have been intentionally or unintentionally used, for example sands, soils and rocks [1]. Young's modulus of enamels from the occlusal surface to the enamel–dentin junction (EDJ) was found to be a graded one, and the crystal orientation linking with the graded behavior of enamels has an important role in promoting shear deformation and dissipating indentation energy [31]. Therefore, it is quite necessary to make a deep exploration into the contact behavior of FGMs with arbitrarily oriented gradient properties.

The "incomplete" or the convex contact model between a cylindrical punch and an elastic half-plane with an arbitrary gradient direction has been investigated [32]. What is about a complete model [33] since stress singularity would emerge unavoidably near the two contact edges? In this paper, a complete contact model between a rigid flat punch and an FGM substrate with the shear modulus varying exponentially in an arbitrary orientation is studied. With the help of Fourier integral transform method, the proposed contact problem reduces to a singular integral equation of the second kind. Numerical calculations give the contact stress distributions and the corresponding stress singularities. The effect of different parameters on contact stresses is further studied in out in order to assess the surface wear resistance.

2 Contact model and theoretical analysis

The plane contact model considered in the present paper is shown in Fig. 1, where a rigid flat punch contacts frictionally with a graded half-plane. The shear modulus of the half-plane varies exponentially in y' direction as shown in Fig. 1. θ, the angle between x-axis and x'-axis, represents the orientation of the gradient. The contact length extends from $x = -a$ to $x = b$ at $y = 0$. P is the normal force acted on the rigid punch in y direction, and Q denotes the frictional force in the contact region in x direction. The normal and tangential forces abide by the Coulomb-type law, i.e.,

$$Q = \mu_{\mathrm{f}} P, \tag{1}$$

where μ_{f} is the friction coefficient and assumed to be a constant.

The graded shear modulus μ of the half-plane can be expressed as

$$\mu(y') = \mu_0 \mathrm{e}^{\delta y'}, \tag{2}$$

in the (x', y') coordinate system, or

$$\mu(x, y) = \mu_0 \mathrm{e}^{\beta x + \gamma y}, \tag{3}$$

in the (x, y) coordinate system, where

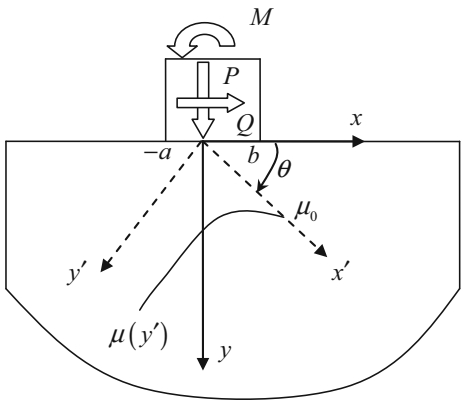

Fig. 1 Schematic of a contact model involving a rigid flat punch of width $(a+b)$ in a frictional contact with a graded half-plane, the gradient orientation of whose shear modulus is in the direction of y' axis and is represented by an angle θ

$$\beta = -\delta \sin\theta = -\frac{\delta \tan\theta}{\sqrt{1+\tan^2\theta}}, \tag{4}$$

$$\gamma = \delta \cos\theta = \frac{\delta}{\sqrt{1+\tan^2\theta}}. \tag{5}$$

The subscript "0" denotes the surface layer. μ_0 and δ are two material constants. Poisson's ratio of the graded half-plane is assumed to be a constant.

$u(x, y)$ and $v(x, y)$ denote the displacement components in the x and y directions, respectively. The constitutive relations of the graded half-plane in terms of the displacement components are given as

$$\sigma_{xx} = \frac{\mu}{\kappa-1}\left[(1+\kappa)\frac{\partial u}{\partial x} + (3-\kappa)\frac{\partial v}{\partial y}\right], \tag{6.1}$$

$$\sigma_{yy} = \frac{\mu}{\kappa-1}\left[(1+\kappa)\frac{\partial v}{\partial y} + (3-\kappa)\frac{\partial u}{\partial x}\right], \tag{6.2}$$

$$\sigma_{xy} = \mu\left[\frac{\partial u}{\partial y} + \frac{\partial v}{\partial x}\right] \tag{6.3}$$

where σ_{xx}, σ_{xy} and σ_{yy} are stress components in the half-plane induced by the pressed punch. $\kappa = 3-4\nu$ for a plane strain model and $\kappa = (3-\nu)/(1+\nu)$ for a plane stress one.

The corresponding equilibrium equations can be written as

$$\begin{aligned}(\kappa+1)\frac{\partial^2 u}{\partial x^2} + (\kappa-1)\frac{\partial^2 u}{\partial y^2} + 2\frac{\partial^2 v}{\partial x \partial y} + \beta(\kappa+1)\frac{\partial u}{\partial x}\\ +\gamma(\kappa-1)\frac{\partial u}{\partial y} + \gamma(\kappa-1)\frac{\partial v}{\partial x} + \beta(3-\kappa)\frac{\partial v}{\partial y} = 0,\end{aligned} \tag{7.1}$$

$$\begin{aligned}(\kappa-1)\frac{\partial^2 v}{\partial x^2} + (\kappa+1)\frac{\partial^2 v}{\partial y^2} + 2\frac{\partial^2 u}{\partial x \partial y} + \gamma(3-\kappa)\frac{\partial u}{\partial x}\\ +\beta(\kappa-1)\frac{\partial u}{\partial y} + \beta(\kappa-1)\frac{\partial v}{\partial x} + \gamma(\kappa+1).\frac{\partial v}{\partial y} = 0.\end{aligned} \tag{7.2}$$

For the special case of a homogeneous half-plane we have $\delta = 0$, $\beta = 0$, $\gamma = 0$.

3 Boundary conditions

For a rigid flat punch, the normal displacement in the contact region is known a priori, i.e.,

$$v(x, 0) = h, \quad -a \le x \le b \tag{8}$$

where h denotes the penetration depth of the rigid flat punch into the half-plane. The normal and tangential tractions in the contact region abide by the Coulomb friction law, i.e.,

$$\sigma_{xy}(x,0) = \mu_{\mathrm{f}}\sigma_{yy}(x,0), \quad -a \le x \le b. \tag{9}$$

The equilibrium conditions of force P and moment M lead to

$$\int_{-a}^{b} \sigma_{yy}(x,0)\mathrm{d}x = -P, \qquad -a \le x \le b, \tag{10}$$

$$\int_{-a}^{b} x\sigma_{yy}(x,0)\mathrm{d}x = -M, \quad -a \le x \le b. \tag{11}$$

Outside the contact region, we have

$$\sigma_{yy}(x,0) = \sigma_{xy}(x,0) = 0, \qquad x < -a, x > b, \tag{12}$$

and the normal and tangential displacements vanish if $y \to +\infty$, i.e.,

$$u(x,+\infty) = v(x,+\infty) = 0. \tag{13}$$

4 Solutions of the contact stress and the stress intensity factor

Similar to Chen and Chen [22], displacement fields $u(x, y)$ and $v(x, y)$ can be obtained with the help of Fourier integral transform method as

$$\begin{aligned}\frac{\partial u(x,0)}{\partial x} &= \frac{\kappa-1}{4}\frac{\sigma_{yy}(x,0)}{\mu} - \frac{\kappa+1}{4\pi}\int_{-a}^{b}\frac{1}{r-x}\frac{\sigma_{xy}(r,0)}{\mu}\mathrm{d}r \\ &+\frac{1}{\pi}\int_{-a}^{b}\left[K_{11}(x,r)\frac{\sigma_{xy}(r,0)}{\mu} + K_{12}(x,r)\frac{\sigma_{yy}(r,0)}{\mu}\right]\mathrm{d}r,\end{aligned} \tag{14}$$

$$\begin{aligned}\frac{\partial v(x,0)}{\partial x} &= -\frac{\kappa-1}{4}\frac{\sigma_{xy}(x,0)}{\mu} - \frac{\kappa+1}{4\pi}\int_{-a}^{b}\frac{1}{r-x}\frac{\sigma_{yy}(r,0)}{\mu}\mathrm{d}r \\ &+\frac{1}{\pi}\int_{-a}^{b}\left[K_{21}(x,r)\frac{\sigma_{xy}(r,0)}{\mu} + K_{22}(x,r)\frac{\sigma_{yy}(r,0)}{\mu}\right]\mathrm{d}r\end{aligned} \tag{15}$$

where $K_{ij}(x,r)$ are kernel functions shown in the "Appendix."

We rewrite the surface tractions inside the contact area as

$$\sigma_{yy}(x,0) = -p(x), \qquad -a \le x \le b, \tag{16}$$

$$\sigma_{xy}(x,0) = -\mu_{\mathrm{f}}p(x), \quad -a \le x \le b \tag{17}$$

where $p(x)$ denotes the normal traction.

Using these relations and Eqs. (8) and (15) can be one obtains

$$\frac{\kappa-1}{4}\frac{\mu_{\mathrm{f}}p(x)}{\mu} + \frac{1+\kappa}{4\pi}\int_{-a}^{b}\frac{1}{r-x}\frac{p(r)}{\mu}\mathrm{d}r - \frac{1}{\pi}\int_{-a}^{b}Q_1(x,r)\frac{p(r)}{\mu}\mathrm{d}r = 0 \tag{18}$$

where the bounded kernel $Q_1(x,r)$ is given by

$$Q_1(x,r) = \mu_{\mathrm{f}}K_{21}(x,r) + K_{22}(x,r). \tag{19}$$

Introducing the following non-dimensional quantities to solve Eqs. (18) and (10):

$$x = \frac{a+b}{2}s + \frac{b-a}{2}, r = \frac{a+b}{2}t + \frac{b-a}{2}, -a \le (x,r) \le b, -1 \le (s,t) \le 1, \tag{20}$$

$$P_1(x) = \frac{p(x)}{\exp(\beta x)} = -\frac{\sigma_{yy}(x,0)}{\exp(\beta x)} = \tilde{P}_1(s) \tag{21}$$

results in

$$\frac{\kappa-1}{1+\kappa}\mu_{\mathrm{f}}\bar{P}_1(s)+\frac{1}{\pi}\int_{-1}^{1}\frac{\bar{P}_1(t)}{t-s}\mathrm{d}t-\frac{2(a+b)}{\pi(\kappa+1)}\int_{-1}^{1}Q_1(s,t)\bar{P}_1(t)\mathrm{d}t=0, \tag{22}$$

$$\int_{-1}^{1}\bar{P}_1(t)\exp\left[\beta\cdot\left(\frac{a+b}{2}t+\frac{b-a}{2}\right)\right]\mathrm{d}t=-2 \tag{23}$$

where

$$\bar{P}_1(x)=\frac{\tilde{P}_1(s)}{P/(a+b)}. \tag{24}$$

Since the Cauchy-type singular kernel is included in the integral equation (22), the solution can be expressed in terms of Jacobi Polynomials,

$$\bar{P}_1(s)=w(s)\sum_{j=0}^{\infty}A_j P_j^{(\beta_1,\beta_2)}(s),\quad |s|\le 1, \tag{25}$$

in which the weight function $w(s)=(1-s)^{\beta_1}(1+s)^{\beta_2}$, A_j are unknown parameters, and $P_j^{(\beta_1,\beta_2)}(\cdot)$ are Jacobi Polynomials corresponding to the weight function $w(s)$. The superscripts β_1 and β_2 are determined from the physics of the problem [22],

$$\begin{aligned}
&\xi>0: \quad \beta_1=-\tfrac{\varepsilon}{\pi} \qquad \beta_2=\tfrac{\varepsilon}{\pi}-1,\\
&\xi=0: \quad \beta_1=-\tfrac{1}{2} \qquad \beta_2=-\tfrac{1}{2},\\
&\xi<0: \quad \beta_1=\tfrac{\varepsilon}{\pi}-1 \quad \beta_2=-\tfrac{\varepsilon}{\pi}
\end{aligned} \tag{26}$$

where $\xi=\frac{\kappa-1}{1+\kappa}\mu_{\mathrm{f}}$, $\tan\varepsilon=|\frac{1}{\xi}|$. It is easy to find that β_1 and β_2 as indexes of stress singularities at the leading $(x=b)$ and trailing $(x=-a)$ contact edges, respectively, depend only on the friction coefficient and Poisson's ratio.

Taking into consideration the following property of Jacobi Polynomials:

$$\begin{aligned}
&\mu_{\mathrm{f}}\tfrac{\kappa-1}{1+\kappa}w(s)P_j^{(\beta_1,\beta_2)}(s)+\tfrac{1}{\pi}\int_{-1}^{1}\frac{1}{s-t}w(t)P_j^{(\beta_1,\beta_2)}(t)\mathrm{d}t \qquad |s|\le 1\\
&=-\tfrac{2^{-1}}{\sin(\pi\beta_1)}P_{j-1}^{(-\beta_1,-\beta_2)}(s),
\end{aligned} \tag{27}$$

and substituting Eq. (25) into Eqs. (22) and (23) yields

$$\sum_{j=1}^{\infty}\left[\frac{-1}{2\sin(\pi\beta_1)}P_{j-1}^{(-\beta_1,-\beta_2)}(s)+Q_j^*(s)\right]A_j=0, \tag{28}$$

$$\int_{-1}^{1}\sum_{j=0}^{\infty}w(t)P_j^{(-\beta_1,-\beta_2)}(t)\exp\left\{\frac{\beta}{2}[(a+b)t+(b-a)]\right\}A_j\mathrm{d}t=-2 \tag{29}$$

where

$$Q_j^*(s)=-\frac{2(a+b)}{\pi(\kappa+1)}\int_{-1}^{1}Q_1(s,t)w(t)P_j^{(\beta_1,\beta_2)}(t)\mathrm{d}t. \tag{30}$$

Considering the following orthogonality property of Jacobi Polynomials:

$$\int_{-1}^{1}w(t)P_j^{(\beta_1,\beta_2)}(t)P_k^{(\beta_1,\beta_2)}(t)\mathrm{d}t=\theta_j^{(\beta_1,\beta_2)}\delta_{jk},\quad j,k=0,1,2,\ldots \tag{31}$$

where

$$\theta_j^{(\beta_1,\beta_2)} = \begin{cases} \int_{-1}^{1} w(t)\mathrm{d}t = \frac{2^{\beta_1+\beta_2+1}\Gamma(\beta_1+1)\Gamma(\beta_2+1)}{\Gamma(\beta_1+\beta_2+2)}, & j=0, \\ \frac{2^{\beta_1+\beta_2+1}\Gamma(j+\beta_1+1)\Gamma(j+\beta_2+1)}{(2j+\beta_1+\beta_2+1)j!\Gamma(j+\beta_1+\beta_2+1)}, & j\geq 1, \end{cases} \tag{32}$$

δ_{jk} is the Kronecker delta function, truncating the series in Eqs. (28) and (29) at $j = N$, and selecting collocation points s_m ($m = 1, 2, \ldots, N$), as roots of the following Jacobi Polynomials:

$$P_N^{(-\beta_1,-\beta_2)}(s_m) = 0 \tag{33}$$

yields

$$-\frac{\theta_j^{(-\beta_1,-\beta_2)}}{2\sin(\pi\beta_1)}A_{j+1} + \sum_{k=0}^{N} d_{jk}A_j = 0, \tag{34.1}$$

$$\int_{-1}^{1}\sum_{j=0}^{N} w(t)P_j^{(-\beta_1,-\beta_2)}(t)\exp\left\{\frac{\beta}{2}[(a+b)t+(b-a)]\right\}A_j dt = -2 \tag{34.2}$$

where

$$d_{jk} = \int_{-1}^{1} Q_j^*(s)P_k^{(-\beta_1,-\beta_2)}(s)(1-s)^{-\beta_1}(1+s)^{-\beta_2}\mathrm{d}s. \tag{35}$$

It is found that Eq. (34) consists of $N + 1$ linear algebraic equations for $N + 1$ unknown constants A_j ($j = 0, 1, \ldots, N$). Based on the solution, $p(x)$ in Eq. (21) can be approximately given as

$$p(x) = \frac{P\exp(\beta x)}{a+b}\left(1-\frac{2x-(b-a)}{a+b}\right)^{\beta_1}\left(1+\frac{2x-(b-a)}{a+b}\right)^{\beta_2}\sum_{j=0}^{N}A_j P_j^{(\beta_1,\beta_2)}\left(\frac{2x-(b-a)}{a+b}\right). \tag{36}$$

Then, the expression for the in-plane stress component $\sigma_{xx}(x, 0)$ under the flat punch can be obtained from the constitutive relations in Eq. (6) and Eqs. (14) and (15) as

$$\begin{aligned}\sigma_{xx}(x,0) = -p(x) + \frac{2\mu_{\mathrm{f}}}{\pi}\int_{-a}^{b}\frac{1}{r-x}p(r)\mathrm{d}r \\ -\frac{8}{\pi(\kappa+1)}\int_{-a}^{b}Q_2(x,r)p(r)\mathrm{d}r,\end{aligned} \qquad |x| < \infty \tag{37}$$

where

$$Q_2(x,r) = K_{11}(x,r) + \mu_{\mathrm{f}}K_{12}(x,r). \tag{38}$$

Stress intensity factors near the contact edges can be defined as

$$K_{\mathrm{I}}(-a) = \lim_{y\to -a}\frac{p(x)}{2^{\beta_1}}(a+x)^{-\beta_2} = \sigma_0\left(\frac{a+b}{2}\right)^{-\beta_2}\sum_{j=0}^{\infty}\frac{A_j P_j^{(\beta_1,\beta_2)}(-1)\exp(-\beta)}{2}, \tag{39}$$

$$K_{\mathrm{I}}(b) = \lim_{y\to b}\frac{p(x)}{2^{\beta_2}}(b-x)^{-\beta_1} = \sigma_0(\frac{a+b}{2})^{-\beta_1}\sum_{j=0}^{\infty}\frac{A_j P_j^{(\beta_1,\beta_2)}(1)\exp(\beta)}{2} \tag{40}$$

where $\sigma_0 = \frac{2P}{(a+b)}$.

5 Discussion of special cases

Closed-form solutions for a rigid flat punch contacting a homogeneous half-plane can be derived from the present model, where we have $a = b$ [2],

$$\frac{\sigma_{yy}(x,0)}{\sigma_0} = \frac{2\sin\pi\beta_1}{\pi}\left(1-\frac{x}{a}\right)^{\beta_1}\left(1+\frac{x}{a}\right)^{\beta_2}, \tag{41}$$

$$\frac{\sigma_{xx}(x,0)}{\sigma_0} = \frac{2\sin\pi\beta_1}{\pi}\begin{cases}\left(1-\frac{x}{a}\right)^{\beta_1}\left(1+\frac{x}{a}\right)^{\beta_2}+\frac{2\mu_f}{\pi}L_f(x), & -a<x<a,\\ \frac{2\mu_f}{\pi}L_f(x), & |x|>a,\end{cases} \tag{42}$$

in which

$$L_f(x) = \begin{cases}-\left(1-\frac{x}{a}\right)^{\beta_1}\left(-1-\frac{x}{a}\right)^{\beta_2}, & -\infty<x<-a,\\ \left(1-\frac{x}{a}\right)^{\beta_1}\left(1+\frac{x}{a}\right)^{\beta_2}\cos\pi\beta_1, & -a<x<a,\\ \left(\frac{x}{a}-1\right)^{\beta_1}\left(1+\frac{x}{a}\right)^{\beta_2}, & a<x<\infty.\end{cases} \tag{43}$$

The stress intensity factors at two symmetric contact edges can be achieved as

$$K_1(a) = -\frac{2\sigma_0}{\pi a^{\beta_1}}\sin\pi\beta_1, \tag{44}$$

$$K_1(-a) = -\frac{2\sigma_0}{\pi a^{\beta_2}}\sin\pi\beta_1. \tag{45}$$

Figure 2 shows the distribution of dimensionless contact stresses $\sigma_{yy}(x,0)/\sigma_0$ and $\sigma_{xx}(x,0)/\sigma_0$, respectively, where σ_0 is the average contact pressure. Figure 2b exhibits an unbounded and discontinuous contact stress

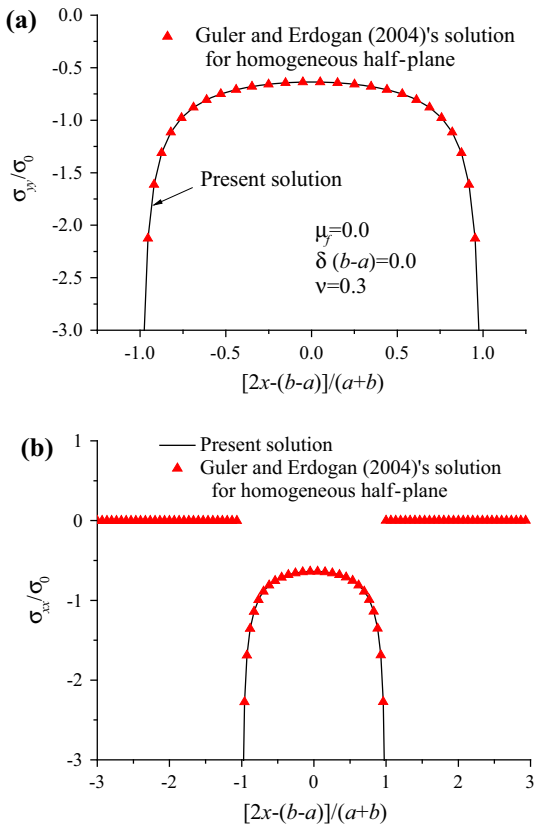

Fig. 2 Distribution of contact stresses for the model of a rigid flat punch on a homogeneous half-plane with determined parameters $\nu = 0.3$, $\delta(b-a) = 0$ and $\mu_f = 0$; **a** for the contact pressure $\sigma_{yy}(x,0)/\sigma_0$; **b** for the in-plane stress $\sigma_{xx}(x,0)/\sigma_0$

Table 1 Non-dimensional stress intensity factors $K_{\mathrm{I}}(-a)/K_{01}$ and $K_{\mathrm{I}}(b)/K_{02}$ at two contact edges in cases of a laterally graded half-plane and a homogeneous one, where $K_{01}=\sigma_0\left(\frac{a+b}{2}\right)^{-\beta_2}$ and $K_{02}=\sigma_0\left(\frac{a+b}{2}\right)^{-\beta_1}$

	Homogeneous half-plane	Laterally graded half-plane ($\delta(a+b)=-0.5$)	
	$\mu_{\mathrm{f}}=0.0$	$\mu_{\mathrm{f}}=0.0$	$\mu_{\mathrm{f}}=0.3$
$K_{\mathrm{I}}(-a)/K_{01}$	0.3183	0.2490	0.2437
$K_{\mathrm{I}}(b)/K_{02}$	0.3183	0.4106	0.4057

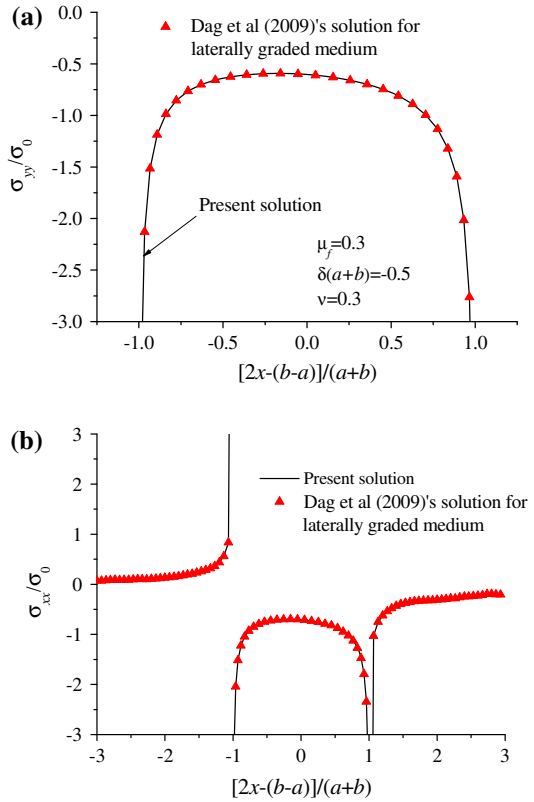

Fig. 3 Distribution of contact stresses for the model of a laterally graded half-plane with fixed parameters $\nu=0.3, \delta(a+b)=-0.5$, $\delta(b-a)=0$ and $\mu_{\mathrm{f}}=0.3$; **a** for the contact pressure $\sigma_{yy}(x,0)/\sigma_0$; **b** for the in-plane stress $\sigma_{xx}(x,0)/\sigma_0$

$\sigma_{xx}(x,0)/\sigma_0$ at both contact edges, which corresponds to the typical characteristic of a rigid flat punch. The non-dimensional stress intensity factors $K_{\mathrm{I}}(-a)/K_{01}$ and $K_{\mathrm{I}}(b)/K_{02}$ are given in Table 1 with $K_{01}=\sigma_0\left(\frac{a+b}{2}\right)^{-\beta_2}$ and $K_{02}=\sigma_0\left(\frac{a+b}{2}\right)^{-\beta_1}$, which shows a good consistence with Guler and Erdogan's predictions [2].

Another special case is $\theta=\pi/2$ for a laterally graded half-plane, we have $\mu(x)=\mu_0 \mathrm{e}^{\delta x}$. Solutions to the contact model of a rigid punch on a laterally graded half-plane can be found based on the present model. Taking the orientation angle $\theta=\frac{\pi}{2}$ and the same material parameters as those in Dag et al. [30] (note that a opposite coordinate has been chosen in the present paper) yields excellent agreement as shown in Fig. 3. Furthermore, the non-dimensional stress intensity factors can be calculated as given in Table 1. From the right column of Table 1, one can see that whether the friction coefficient vanishes or not, the non-dimensional stress intensity factors at both contact edges do not equal in the laterally graded half-plane model, unlike the homogeneous half-plane one.

6 Numerical results and analysis

Due to a negligible effect of the value of Poisson's ratio on the contact behavior [34,35], we take $\nu=0.3$ in all analyses. The above theoretical analysis shows that several factors, such as the friction coefficient, non-

homogeneity and angle of the gradient orientation, should produce influences on the contact behavior, which are discussed in the following Subsection.

6.1 The effect of several factors on the contact behavior

The non-homogeneous feature of a graded half-plane is characterized by three parameters δ, $-a$ and b. It is reasonable to adopt two non-dimensional parameters $\delta(a+b)$ and $\delta(b-a)$ to analyze the numerical results, instead of three separated parameters. Therefore, we take $\delta(a+b)$ as a variable for convenience and $\delta(b-a)=0$ in our numerical results, which means the y-axis goes through the center of the flat punch.

Distributions of the non-dimensional contact pressure $\sigma_{yy}(x,0)/\sigma_0$ and the in-plane surface stress component $\sigma_{xx}(x,0)/\sigma_0$ are shown in Fig. 4a, b, and the stress singularity near both contact edges is given in Table 2 for different friction coefficients μ_{f}. Figure 4a shows that the friction coefficient does not exhibit a significant effect on the magnitude of the contact pressure, but makes the contact pressure asymmetric, and the curve tends to be more oblique for a larger value of μ_{f}. The in-plane surface stress changes from compressive to tensile near the trailing edge ($x<-a$), while it keeps compressive near the leading edge ($x>b$) and becomes stronger along with an increasing friction coefficient as shown in Fig. 4b. The stress singularity becomes stronger at the trailing end (β_2) and weaker at the leading end (β_1) for a larger μ_{f} in Table 2. From the fretting mechanics

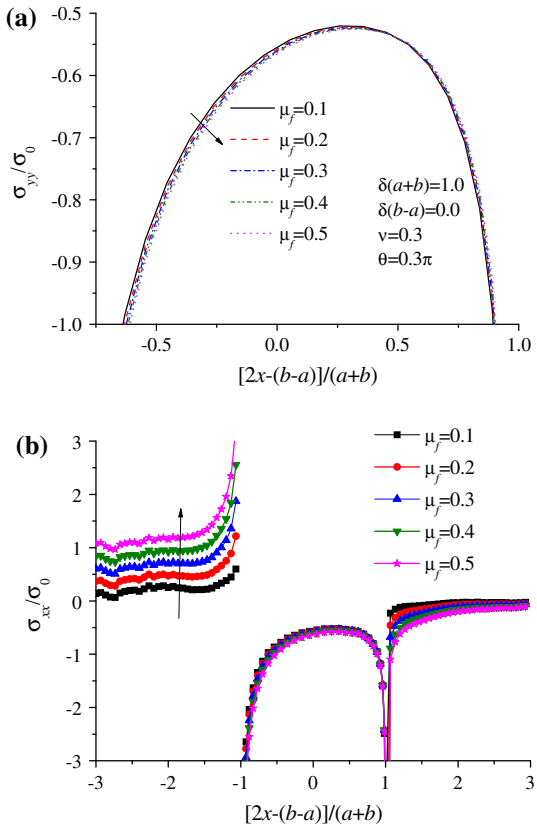

Fig. 4 Distribution of the non-dimensional contact stresses for the model of a graded half-plane with gradient orientation angle $\theta=0.3\pi$ and determined parameters $\nu=0.3$, $\delta(a+b)=1.0$, $\delta(b-a)=0$, but for different friction coefficients; **a** for the contact pressure $\sigma_{yy}(x,0)/\sigma_0$; **b** for the in-plane stress $\sigma_{xx}(x,0)/\sigma_0$

Table 2 Stress singularities β_1, β_2 at two contact edges for different friction coefficients μ_{f} with determined parameters $\theta=0.3\pi$, $\nu=0.3$, $\delta(a+b)=1.0$ and $\delta(b-a)=0$

$\mu_{\mathrm{f}}=0.1$	$\mu_{\mathrm{f}}=0.2$	$\mu_{\mathrm{f}}=0.3$	$\mu_{\mathrm{f}}=0.4$	$\mu_{\mathrm{f}}=0.5$
$\beta_1=-0.4909$	$\beta_1=-0.4818$	$\beta_1=-0.4728$	$\beta_1=-0.4638$	$\beta_1=-0.4548$
$\beta_2=-0.5091$	$\beta_2=-0.5182$	$\beta_2=-0.5272$	$\beta_2=-0.5362$	$\beta_2=-0.5452$

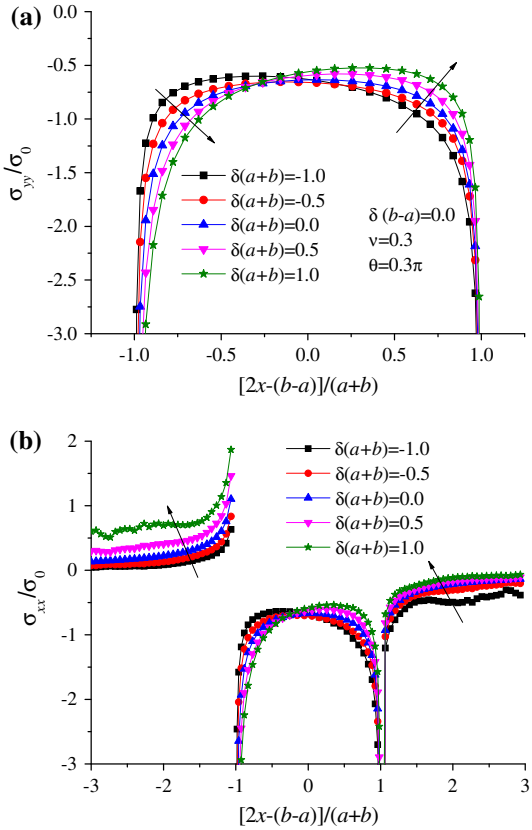

Fig. 5 Distributions of the non-dimensional contact stresses for the model of a graded half-plane with gradient orientation angle $\theta = 0.3\pi$ and determined parameters $\nu = 0.3$, $\mu_f = 0.3$, $\delta(b-a) = 0$, but for different non-homogeneities $\delta(a+b)$; **a** for the contact pressure $\sigma_{yy}(x,0)/\sigma_0$; **b** for the in-plane stress $\sigma_{xx}(x,0)/\sigma_0$

point of view, surface cracking will be inevitable at least near the trailing edge. Therefore, a small friction coefficient is helpful to relieve such contact damages.

The effect of non-homogeneity parameters $\delta(a+b)$ on the contact pressure and the in-plane stress is shown in Fig. 5a, b, respectively, where a positive value of $\delta(a+b)$ implies an increasing shear modulus in the y' gradient direction and a negative value implies a decreasing shear modulus in the gradient direction. The graded half-plane degrades into a homogeneous one for a vanishing $\delta(a+b)$. Figure 5a demonstrates a significant influence of the non-homogeneity on the compressive contact pressure, the absolute value of which increases near the trailing edge and decreases near the leading edge for the value of $\delta(a+b)$ increasing from negative to positive. Variation of the in-plane stress in Fig. 5b clearly shows that a graded half-plane with a decreasing stiffness in the gradient direction, i.e., $\delta(a+b) < 0$, will have less possibility for crack initiation. Such an interesting finding agrees qualitatively with the results in Guler and Erdogan [2] and those in Choi and Paulino [36]. However, an opposite phenomenon was found in Chen and Chen [22] due to different boundary conditions. The results are helpful for understanding the gradient characteristics in many biomaterials, for example teeth and bones.

Figure 6 shows the effect of gradient orientation angles on the contact stress field. Figures 6a, b correspond to cases of a graded half-plane with a decreasing shear modulus in the gradient direction, i.e., $\delta(a+b) < 0$, while Figs. 6c, d correspond to $\delta(a+b) > 0$. No theoretical solution exists for the case of $\delta(a+b) < 0$ and $\theta = 0$ [13], which shows a restriction on the value of gradient orientation angles θ. The curve of the contact pressure becomes much oblique when θ changes from 0.1π to 0.5π with determined values of $\delta(b-a) = 0$ and $\mu_f = 0.3$, as shown in Figs. 6a, c. However, the variation trends of the contact pressure near the trailing and leading edges are contrary for the cases of $\delta(a+b) > 0$ and $\delta(a+b) < 0$. The influence of the gradient orientation angles on the in-plane stress is more obvious ahead of the leading edge than that behind the trailing edge, as shown in Figs. 6b, d. In general, the effect of the gradient orientation angles on the in-plane stress is weak. The corresponding non-dimensional stress intensity factors are listed in Table 3, where the variation

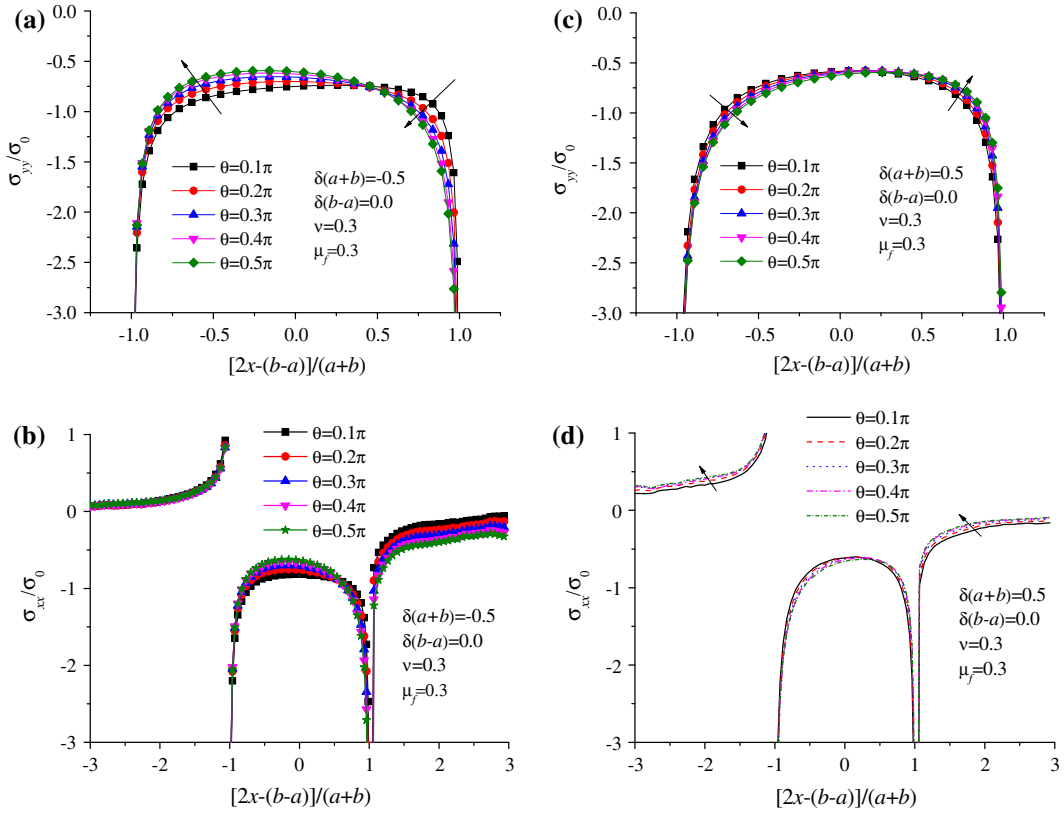

Fig. 6 Distributions of the non-dimensional contact stresses for the model of a graded half-plane with determined parameters $\nu = 0.3$, $\mu_{\mathrm{f}} = 0.3$ and $\delta(b-a) = 0$, but for different gradient orientation angles θ. **a** For the contact pressure $\sigma_{yy}(x,0)/\sigma_0$ with $\delta(a+b) = -0.5$; **b** for the in-plane stress $\sigma_{xx}(x,0)/\sigma_0$ with $\delta(a+b) = -0.5$; **c** for the contact pressure $\sigma_{yy}(x,0)/\sigma_0$ with $\delta(a+b) = 0.5$; **d** for the in-plane stress $\sigma_{xx}(x,0)/\sigma_0$ with $\delta(a+b) = 0.5$

of the stress intensity factors at the leading edge is more regular than that at the trailing edge. In cases of $\delta(a+b) < 0$, the stress intensity factor $K_{\mathrm{I}}(b)/K_{02}$ near the leading edge increases with an increasing θ, while it decreases in cases of $\delta(a+b) > 0$. A surprising result is that the minimum value of $K_{\mathrm{I}}(-a)/K_{01}$ near the trailing edge does not always emerge in a case with a relatively small gradient orientation angle, as given in Table 3. The value of gradient orientation angle θ corresponding to the minimum stress intensity factor seems to depend on $\delta(a+b)$, which is similar to the problem of a mixed crack in a non-homogeneous elastic half-plane [37].

6.2 The moment to keep punches moving perpendicularly to the contact surface

In most of the literatures relevant to a rigid punch contacting a half-plane, an assumption of punches moving perpendicularly to the contact surface is usually adopted by forcing the punch fixed in a rail system [2,4]. However, evaluation of the applied moment is vital for certain practical circumstances [38].

The non-dimensional moment $M/[P(a+b)/2]$ is given in Fig. 7 for various friction coefficients μ_{f} with determined parameters $\theta = 0.3\pi$, $\delta(b-a) = 0$ and $\delta(a+b) = -0.5, 0, 1.0$. The intercept on the vertical coordinate corresponds to the frictionless case. The moment increases monotonously with an increasing friction coefficient, which is due to the severe asymmetry induced by a high friction coefficient.

The effect of non-homogeneity parameters $\delta(a+b)$ and gradient orientation angles θ on the non-dimensional moment $M/[P(a+b)/2]$ is illustrated in Figs. 8 and 9 with $\mu_{\mathrm{f}} = 0.3$, respectively. The result for a homogeneous half-plane case is given for comparison, in which $\delta(a+b) = 0$ and the applied moment vanishes. From Fig. 8, it is observed that the value of the required moment tends to increase significantly with an increasing $\delta(a+b)$ when $\theta \geq 0.15\pi$. However, when $\theta < 0.15\pi$, the monotonous variation does not hold any more as shown in Fig. 9. An interesting phenomenon is that the value of the required moment increases

Table 3 Variations of non-dimensional stress intensity factors $K_{\mathrm{I}}(-a)/K_{01}$, $K_{\mathrm{I}}(b)/K_{02}$ at two contact edges for different combinations of θ and $\delta(a+b)$ with fixed parameters $\mu_{\mathrm{f}}=0.3$, $\nu=0.3$ and $\delta(b-a)=0$

$(a+b)\delta$	θ ($\beta_1=-0.4728$, $\beta_2=-0.5272$)				
	0.1π	0.2π	0.3π	0.4π	0.5π
-1.0					
$K_{\mathrm{I}}(-a)/K_{01}$	0.1077	0.1765	0.1835	0.1799	0.1837
$K_{\mathrm{I}}(b)/K_{02}$	0.2354	0.2810	0.3709	0.4585	0.5114
-0.5					
$K_{\mathrm{I}}(-a)/K_{01}$	0.2597	0.2450	0.2408	0.2393	0.2437
$K_{\mathrm{I}}(b)/K_{02}$	0.2208	0.2815	0.3310	0.3755	0.4057
0					
$K_{\mathrm{I}}(-a)/K_{01}$	0.3171	0.3171	0.3171	0.3171	0.3171
$K_{\mathrm{I}}(b)/K_{02}$	0.3171	0.3171	0.3171	0.3171	0.3171
0.5					
$K_{\mathrm{I}}(-a)/K_{01}$	0.3754	0.3986	0.4141	0.4191	0.4120
$K_{\mathrm{I}}(b)/K_{02}$	0.3373	0.3104	0.2867	0.2675	0.2529
1.0					
$K_{\mathrm{I}}(-a)/K_{01}$	0.4233	0.4766	0.5153	0.5326	0.5241
$K_{\mathrm{I}}(b)/K_{02}$	0.3329	0.2822	0.2425	0.2147	0.1976

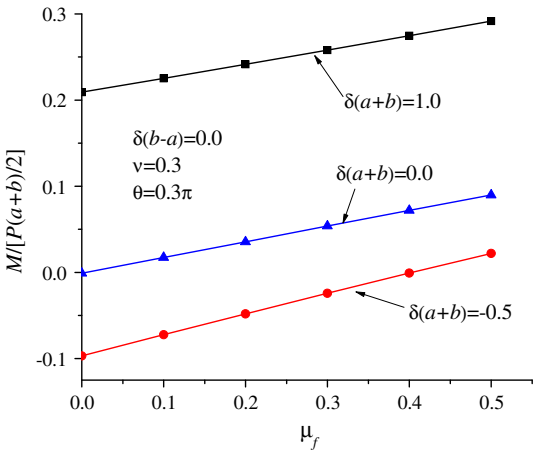

Fig. 7 The non-dimensional required moment $M/[P(a+b)/2]$ as a function of the friction coefficient μ_{f} with determined parameters $\nu=0.3$, $\delta(b-a)=0$, $\theta=0.3\pi$, but for different values of $\delta(a+b)$

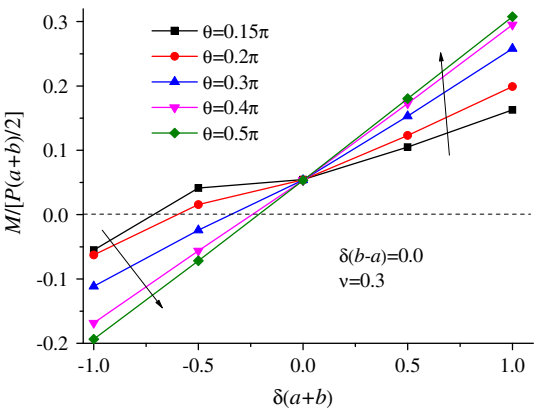

Fig. 8 The non-dimensional required moment $M/[P(a+b)/2]$ as a function of parameter $\delta(a+b)$ with determined parameters $\nu=0.3$, $\delta(b-a)=0$, and $\mu_{\mathrm{f}}=0.3$, but for different gradient orientation angles θ

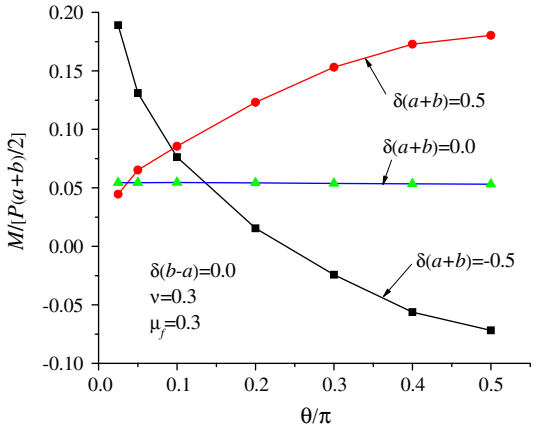

Fig. 9 The non-dimensional required moment $M/[P(a+b)/2]$ as a function of the gradient orientation angle θ with determined parameters $\nu = 0.3$, $\delta(b-a) = 0$, and $\mu_{\mathrm{f}} = 0.3$, but for different values of $\delta(a+b)$

gradually with an increasing gradient orientation angle θ in cases of $\delta(a+b) > 0$, while it decreases and even changes the moment direction in cases of $\delta(a+b) < 0$. It can be inferred that a proper combination of the friction coefficient μ_{f}, non-homogeneity parameter $\delta(a+b)$ and gradient orientation angle θ could reduce or avoid the additionally required moment. All the results further demonstrate that the inner properties of materials have significant effects on their surface behaviors.

7 Conclusions

The frictional contact model of a rigid flat punch on a graded half-plane is analyzed. The shear modulus of the half-plane varies exponentially in an arbitrary direction. Comparing to the homogeneous half-plane case and the laterally graded elastic model one finds that the contact pressure and in-plane surface stress are significantly influenced by the surface friction coefficient, non-homogeneity parameter, and the gradient orientation angle. Stress singularities and the stress intensity factors at both contact edges are obtained. In addition, the required moment to keep the punch moving perpendicularly to the contact surface is evaluated. All the results in the present paper should be helpful for the design of novel graded materials with strong wear resistance and understanding the mechanical mechanism of naturally graded biomaterials.

Acknowledgments The authors thank the support of NSFC (Grant Nos. 11402292, 11404393), Natural Science Foundation of Jiangsu Province (Grant No. BK20140179), and the Fundamental Research Funds for the Central Universities (Grant No. 2014QNA73).

Appendix

The kernels $K_{ij}(x,r)$ in Eqs. (14) and (15) are expressed as

$$K_{11}(x,r) = \int_0^{+\infty} \left[\alpha N_{11}(\alpha) + \frac{\kappa+1}{4}\right] \sin\left[\alpha(r-x)\right] \mathrm{d}\alpha, \tag{A1.1}$$

$$K_{12}(x,r) = -i\int_0^{+\infty} \left[\alpha N_{12}(\alpha) - i\frac{\kappa-1}{4}\right] \cos\left[\alpha(r-x)\right] \mathrm{d}\alpha, \tag{A1.2}$$

$$K_{21}(x,r) = -i\int_0^{+\infty} \left[\alpha N_{21}(\alpha) + i\frac{\kappa-1}{4}\right] \cos\left[\alpha(r-x)\right] \mathrm{d}\alpha, \tag{A1.3}$$

$$K_{22}(x,r) = \int_0^{+\infty} \left[\alpha N_{22}(\alpha) + \frac{\kappa+1}{4}\right] \sin\left[\alpha(r-x)\right] \mathrm{d}\alpha. \tag{A1.4}$$

$N_{jk}(\alpha)$ $(j,k=1,2)$ in the kernels are the elements of $\mathbf{N}(\alpha)$, i.e.,

$$\mathbf{N}(\alpha)=\begin{bmatrix} m_1 & m_2 \\ 1 & 1 \end{bmatrix} \bullet \begin{bmatrix} \mu/(m_1n_1-i\alpha) & \mu/(m_2n_2-i\alpha) \\ \mu/\{(\kappa-1)[-i\alpha m_1(3-\kappa)+n_1(1+\kappa)]\} & \mu/\{(\kappa-1)[-i\alpha m_2(3-\kappa)+n_2(1+\kappa)]\} \end{bmatrix}^{-1} \tag{A2}$$

where

$$n_1(\alpha)=-\frac{\Delta_1}{2}-\frac{\sqrt{\Delta_1^2+4(\alpha^2+i\alpha\Delta_2)}}{2},\quad n_2(\alpha)=-\frac{\Delta_3}{2}-\frac{\sqrt{\Delta_3^2+4(\alpha^2+i\alpha\Delta_4)}}{2}, \tag{A3.1}$$

$$n_3(\alpha)=-\frac{\Delta_1}{2}+\frac{\sqrt{\Delta_1^2+4(\alpha^2+i\alpha\Delta_2)}}{2},\quad n_4(\alpha)=-\frac{\Delta_3}{2}+\frac{\sqrt{\Delta_3^2+4(\alpha^2+i\alpha\Delta_4)}}{2}, \tag{A3.2}$$

$$\Delta_1=\beta\sqrt{\frac{3-\kappa}{\kappa+1}}+\gamma,\quad \Delta_2=\beta-\gamma\sqrt{\frac{3-\kappa}{\kappa+1}},\quad \Delta_3=\gamma-\beta\sqrt{\frac{3-\kappa}{\kappa+1}},\quad \Delta_4=\beta+\gamma\sqrt{\frac{3-\kappa}{\kappa+1}}, \tag{A3.3}$$

and $m_j(\alpha)$ for each $n_j(\alpha)$ $(j=1,\ldots,4)$ can be given as

$$m_j(\alpha)=\frac{[2i\alpha-\beta(3-\kappa)]\,n_j+i(\kappa-1)\alpha\gamma}{(\kappa-1)n_j^2+(\kappa-1)\gamma n_j-(\kappa+1)\alpha(\alpha+i\beta)}. \tag{A4}$$

References

1. Suresh, S.: Graded materials for resistance to contact deformation and damage. Science **292**, 2447–2451 (2001)
2. Guler, M.A., Erdogan, F.: Contact mechanics of graded coatings. Int. J. Solids Struct. **41**, 3865–3889 (2004)
3. Mortensen, A., Suresh, S.: Fundamentals of Functionally Graded Materials: Processing and Thermomechanical Behaviour of Graded Metals and Metal-Ceramic Composites. IOM Communications Ltd, London, pp. 1–70 (1998)
4. Guler, M.A., Erdogan, F.: The frictional sliding contact problems of rigid parabolic and cylindrical stamps on graded coatings. Int. J. Mech. Sci. **49**, 161–182 (2007)
5. Mishina, H., Inumaru, Y., Kaitoku, K.: Fabrication of ZrO2/AISI316L functionally graded materials for joint prostheses. Mater. Sci. Eng. A-Struct. Mater. **475**, 141–147 (2008)
6. Pender, D.C., Padture, N.P., Giannakopoulos, A.E., Suresh, S.: Gradients in elastic modulus for improved contact-damage resistance. Part I: the silicon nitride–oxynitride glass system. Acta Mater. **49**, 3255–3262 (2001)
7. Pender, D.C., Thompson, S.C., Padture, N.P., Giannakopoulos, A.E., Suresh, S.: Gradients in elastic modulus for improved contact-damage resistance. Part II: the silicon nitride–silicon carbide system. Acta Mater. **49**, 3263–3268 (2001)
8. Suresh, S., Olsson, M., Giannakopoulos, A.E., Padture, N.P., Jitcharoen, J.: Engineering the resistance to sliding-contact damage through controlled gradients in elastic properties at contact surfaces. Acta Mater. **47**, 3915–3926 (1999)
9. Suresh, S., Giannakopoulos, A.E., Alcala, J.: Spherical indentation of compositionally graded materials: theory and experiments. Acta Mater. **45**, 1307–1321 (1997)
10. Jorgensen, O., Giannakopoulos, A.E., Suresh, S.: Spherical indentation of composite laminates with controlled gradients in elastic anisotropy. Int. J. Solids Struct. **35**, 5097–5113 (1998)
11. Krumova, M., Klingshirn, C., Haupert, F., Friedrich, K.: Microhardness studies on functionally graded polymer composites. Compos. Sci. Technol. **61**, 557–563 (2001)
12. Giannakopoulos, A.E., Pallot, P.: Two-dimensional contact analysis of elastic graded materials. J. Mech. Phys. Solids **48**, 1597–1631 (2000)
13. Dag, S., Erdogan, F.: A surface crack in a graded medium loaded by a sliding rigid stamp. Eng. Fract. Mech. **69**, 1729–1751 (2002)
14. Choi, H.J., Paulino, G.H.: Interfacial cracking in a graded coating/substrate system loaded by a frictional sliding flat punch. Proc. R. Soc. A-Math. Phys. Eng. Sci. **466**, 853–880 (2010)
15. El-Borgi, S., Abdelmoula, R., Keer, L.: A receding contact plane problem between a functionally graded layer and a homogeneous substrate. Int. J. Solids Struct. **43**, 658–674 (2006)
16. Elloumi, R., Kallel-Kamoun, I., El-Borgi, S.: A fully coupled partial slip contact problem in a graded half-plane. Mech. Mater. **42**, 417–428 (2010)
17. Ke, L.-L., Wang, Y.-S.: Two-dimensional contact mechanics of functionally graded materials with arbitrary spatial variations of material properties. Int. J. Solids Struct. **43**, 5779–5798 (2006)
18. Liu, T.J., Wang, Y.S.: Axisymmetric frictionless contact problem of a functionally graded coating with exponentially varying modulus. Acta Mech. **199**, 151–165 (2008)
19. Hills, D.A., Nowell, D., Sackfield, A.: Mechanics of Elastic Contacts. Butterworth-Heinemann, Oxford (1993)

20. Nowell, D., Hills, D.A.: Contact problems incorporating elastic layers. Int. J. Solids Struct. **24**, 105–115 (1988)
21. Chen, P., Chen, S.: Contact behaviors of a rigid punch and a homogeneous half-space coated with a graded layer. Acta Mech. **223**, 563–577 (2012)
22. Chen, P., Chen, S.: Thermo-mechanical contact behavior of a finite graded layer under a sliding punch with heat generation. Int. J. Solids Struct. **50**, 1108–1119 (2013)
23. Chen, P., Chen, S., Peng, Z.: Thermo-contact mechanics of a rigid cylindrical punch sliding on a finite graded layer. Acta Mech. **223**, 2647–2665 (2012)
24. Chen, S.H., Yan, C., Soh, A.: Adhesive behavior of two-dimensional power-law graded materials. Int. J. Solids Struct. **46**, 3398–3404 (2009)
25. Chen, S.H., Yan, C., Zhang, P., Gao, H.J.: Mechanics of adhesive contact on a power-law graded elastic half-space. J. Mech. Phys. Solids **57**, 1437–1448 (2009)
26. Jin, F., Guo, X.: Non-slipping adhesive contact of a rigid cylinder on an elastic power-law graded half-space. Int. J. Solids Struct. **47**, 1508–1521 (2010)
27. Jin, F., Guo, X.: Mode-mixity-dependent adhesion of power-law graded elastic solids under normal load and substrate stretch-induced mismatch strain. Int. J. Solids Struct. **49**, 2349–2357 (2012)
28. Jin, F., Guo, X., Gao, H.: Adhesive contact on power-law graded elastic solids: the JKR–DMT transition using a double-Hertz model. J. Mech. Phys. Solids **61**, 2473–2492 (2013)
29. Guo, X., Jin, F., Gao, H.J.: Mechanics of non-slipping adhesive contact on a power-law graded elastic half-space. Int. J. Solids Struct. **48**, 2565–2575 (2011)
30. Dag, S., Guler, M.A., Yildirim, B., Cihan Ozatag, A.: Sliding frictional contact between a rigid punch and a laterally graded elastic medium. Int. J. Solids Struct. **46**, 4038–4053 (2009)
31. O'Brien, S., Shaw, J., Zhao, X., Abbott, P.V., Munroe, P., Xu, J., Habibi, D., Xie, Z.: Size dependent elastic modulus and mechanical resilience of dental enamel. J. Biomech. **5**, 1060–1066 (2014)
32. Chen, P., Chen, S., Peng, J.: Sliding contact between a cylindrical punch and a graded half-plane with an arbitrary gradient direction. J. Appl. Mech.-Trans. ASME **82**, 041008 (2015)
33. Ramesh, R., Hills, D.: Recent progress in understanding the properties of elastic contacts. Proc. Inst. Mech. Eng. Part C-J. Eng. Mech. Eng. Sci. 0954406214556667 (2014)
34. Giannakopoulos, A.E., Suresh, S.: Indentation of solids with gradients in elastic properties. 1. Point force. Int. J. Solids Struct. **34**, 2357–2392 (1997)
35. Giannakopoulos, A.E., Suresh, S.: Indentation of solids with gradients in elastic properties. 2. Axisymmetric indentors. Int. J. Solids Struct. **34**, 2393–2428 (1997)
36. Choi, H.J., Paulino, G.H.: Thermoelastic contact mechanics for a flat punch sliding over a graded coating/substrate system with frictional heat generation. J. Mech. Phys. Solids **56**, 1673–1692 (2008)
37. Konda, N., Erdogan, F.: The mixed mode crack problem in a nonhomogeneous elastic medium. Eng. Fract. Mech. **47**, 533–545 (1994)
38. Galin, L.A.: Contact Problems: The Legacy of LA Galin. Springer, Berlin (2008)